

All-optical periodic code matching by a single-shot frequency-domain cross-correlation measurement

Lev Chuntunov, Leonid Rybak, Andrey Gandman, and Zohar Amitay*

Schulich Faculty of Chemistry, Technion - Israel Institute of Technology, Haifa 32000, Israel

Abstract

Optical single-shot measurement of the cross-correlation function between periodic sequences is demonstrated. The sequences are encoded into the broadband ultrashort phase-shaped pulses which are mixed in the nonlinear medium with additional amplitude-shaped narrowband pulse. The spectrum of the resulted four wave mixing signal is measured to provide the cross-correlation function. The high contrast between the values of cross-correlation and auto-correlation (the latter includes also the information of the sequence period) has potential to be employed in the optical implementation of CDMA communication protocol.

PACS numbers:

*Electronic address: amitayz@tx.technion.ac.il

Modern communication technology, including the mobile 3G wide-band and Global Positioning System standards, implemented in the rf-regime, extensively employs communication based on the Code Division Multiple Access (CDMA) protocol [1]. It is known to be preferable over the Time Division and Frequency Division multiplexing strategies, where different time or frequency slots, respectively, are assigned to different users sharing the common communication channel. In CDMA the transmitter and receiver are assigned a unique code to recognize each other from the overall information flow. The codes are converted into the individual characteristics of different frequency components of the broadband spectrum and translated to the time-dependence of the waveform. This highly efficient spread spectrum multiplexing strategy is potentially capable to support a high number of users, given a large codes families with low correlation properties are available [2]. These code families, thus, must support sufficient number of users, while minimizing the interference between them. The state of the art code families [3, 4, 5] incorporate periodic cyclically distinct pseudo-random sequences over the arbitrary alphabet. The codes have low correlating properties which imply minimal interference between them. This generalization to the extended alphabet dramatically improved the capacity and performance of the CDMA networks, while in the past only the binary codes were considered.

It was recognized several decades ago that the developments of the communication technology in the rf region are also applicable for the optical communication [6, 7]. In the optical implementation the codes are spread over the broad bandwidth of the light pulses, which are phase-shaped in the frequency-domain [8]. Recently, the demand for the fast and reliable multiuser communication stimulated an extensive research activity in this field, focusing on different aspects of optical networking [6, 7]. Availability of a powerful technique to discriminate between different codes is critical to fully benefit from the advantages of CDMA [9, 10]. Here we demonstrate efficient all-optical experimental recognition of matching codes from the large family using single-shot measurement of their entire cross-correlation function in the frequency-domain. The interference between the photo-induced optical pathways excited with two encoded broadband pulses and one amplitude-shaped narrowband pulse within the non-linear medium is employed to evaluate the cross-correlation function between the codes. We utilize the BOXCARs setup [11] to obtain spatially-resolved background-free four-wave-mixing spectrum which is formally equivalent to the cross-correlation function between the codes of interest. Our approach enables the high-contrast discrimination between

the periodic low-correlating codes based on identification of the constructive interference corresponding to the pulses shaped with similar codes and destructive interference corresponding to the pulses shaped with different codes. As opposed to the previously developed techniques [9, 10], the presented setup enables single-shot measurement of the entire cross-correlation function, which in addition provides useful information on the unknown period of the code without additional computational expenses.

We consider the families of periodic cyclically distinct pseudo-random sequences $s_k(t)$ over the alphabet of integers of size p [$0 \leq s_k(t) \leq p-1$] with arithmetics modulo p , where $p \geq 2$. The cross-correlation function between two sequences is defined by

$$c(k, r, \tau) = \sum_{t=0}^{L-1} \omega_p^{s_k(t+\tau) - s_r(t)}, \quad (1)$$

where k and r are indexes of the sequences in the set of size M , $0 \leq \tau \leq L-1$, L - is the period of the sequence, and $\omega_p = e^{i2\pi/p}$ - is p th root of unity. The commonly used merit factor of the codes performance is the maximal value of the correlation $C_{max} = \max\{c(k, r, \tau)\}$ excluding the cases where simultaneously $k = r$ and $\tau=0$, for which, trivially, $C_{max} = L$. We thus demand $C_{max} \ll L$ to ensure the non-intercepted communication with the absence of interference. The nested chain low-correlation codes families $S(0) \subseteq S(1) \subseteq S(2) \subseteq \dots$ obey the desired requirements [3, 4, 5]. For a given period L , the code family of higher order incorporate more code sequences, while the corresponding value of C_{max} increases. However, as the code period L increases, the number of available codes increases, while the value of C_{max} decreases. The C_{max} values of the S -families have a well defined bounds and distribution, and thus can be appropriately tailored to the implementation needs by the choice of L and the order of the family.

In the optical domain, the common implementation of the CDMA network communication involves broadband ultra-fast shaped laser pulses. The high popularity of this benchmark system is mainly due to the Weiner-Heritage design of the pulse shaping apparatus that is used to assign the codes to the laser pulses carrying the transmitted data. The 4f optical setup of the pulse shaper incorporates pixelated liquid crystal Spatial Light Modulator (SLM) in its focal plane, where each spectral component of the laser electric field $E(\omega) = |E(\omega)| e^{i\Phi(\omega)}$ is addressed individually. Here, $|E(\omega)|$ - is the spectral amplitude at frequency ω , and $\Phi(\omega)$ - is the corresponding phase. The phase-shaping is implemented via control over the voltage applied to different pixels of liquid crystal, which induces different phase

retardation of the transmitted light. We assume that spectral segment of $\Delta\omega$ is spread along each pixel. The similarity between the representation of integer code sequences $s_k(\tau)$ in the complex plane and the phase factor of the electric field is used to convert the codes into the relative phases of the broadband pulse spectral components: $\Phi(\omega) = (2\pi/p)s_k(\omega)$. Once the encoding process is completed at the transmitter site, measurement of the cross-correlation function $c(k, r, \tau)$ is the important step that should be performed at the receiver or router site.

Naturally, the single-shot all-optical cross-correlation measurement is the ideal way to effectively discriminate between different codes and identify their period. Translation of the codes into the phases of the pulse spectral components allows one to take advantage of the interference between multiple photo-induced multi-photon pathways excited in the non-linear medium by the broadband pulse. The cross-correlation function $c(k, r, \tau)$ between the two codes s_k and s_r converted into the phases $\Phi_k(\omega)$ and $\Phi_r(\omega)$ of the pulses with the electric fields $E_k(\omega)$ and $E_r(\omega)$ obtains the form of

$$\xi(k, r, \Delta) = \int_{-\infty}^{\infty} E_k(\omega) E_r^*(\omega + \Delta) d\omega = \int_{-\infty}^{\infty} |E_k(\omega)| \cdot |E_r(\omega + \Delta)| e^{i[\Phi_k(\omega) - \Phi_r(\omega + \Delta)]} d\omega. \quad (2)$$

Neglecting the spectral envelope profiles of $|E_{k,r}(\omega)|$, $\xi(k, r, \Delta)$ is formally equivalent to $c(k, r, \tau)$, differing from it by Δ being continuous variable representing detuning between spectral components of $E_k(\omega)$ and $E_r(\omega + \Delta)$, while τ is a discrete integer variable representing the relative delay between the two codes.

Physically, $\xi(k, r, \Delta)$ interferes all the possible two-photon pathways of one absorbed photon and one emitted photon which spectral components are detuned by Δ within the Raman-type process. Suppose that variable ω is divided to small bins of size $\Delta\omega$ and each bin is associated with specific value of t - the index of the code component, so that the phase $\Phi(\omega)$ of the electric field $E(\omega)$ is constant across each bin. For simplicity, we analyze first the case where the spectral envelope is extremely slow and can be approximated to be constant: $|E_{k,r}(\omega)| \simeq 1$. Similar to $c(k, r, \tau)$, $\xi(k, r, \Delta)$ obtains its maximal values when $\Delta = n\Delta\omega L$ if $k = r$, as the interference between all the corresponding two-photon pathways is fully constructive. Here $n = 0, 1, 2 \dots$ and L is the period of the code. For $\Delta \neq n\Delta\omega L$ or $k \neq r$ the interference between the two-photon pathways is destructive and the value of $\xi(k, r, \Delta) \ll \xi(k, k, n\Delta\omega L)$. Overall, the profile of $\xi(k, r, \Delta)$ has peaks corresponding to the cases of the constructive interference that appear with the spacing associated with the period

of $\Delta\omega L$. If the interference is destructive, for the case of flat spectral profiles of $E_{k,r}(\omega)$, the bounds on the value of $\xi(k, r, \Delta)$ are obtained from the results of analysis of $c(k, r, \tau)$ within the framework of Number Theory [3, 4, 5]. For the proper choice of the codes family, these interference is kept sufficiently low and enables clear discrimination between the matching $[k = r]$ and non-matching $[k \neq r]$ codes.

Experimentally, multiple two-photon pathways are interfered within the non-linear medium. However, due to its Raman nature, the presented two-photon photo-excitation is not applicable for the single-shot detection. The latter is possible employing the four-wave mixing process within the medium having third-order susceptibility $\chi^{(3)}$. The interaction includes absorption of two-photons and emission of one photon provided by the excitation electric fields of the lasers, while the fourth emitted photon generated by the non-linear polarization of the medium is detected:

$$E_{sig}(\omega) \propto \int_{-\infty}^{\infty} E_{pump}(\omega') d\omega' \int_{-\infty}^{\infty} E_k(\omega'') E_r^*(\omega'' + \omega' - \omega) d\omega''. \quad (3)$$

To avoid the broadening of the interference pattern created by the pulses $E_k(\omega)$ and $E_r(\omega)$ due to the presence of the additional broadband pump laser pulse $E_{pump}(\omega)$, the latter must be of narrow bandwidth. Let us assume that

$$E_{pump}^{narrow}(\omega) = \int_{-\infty}^{\infty} E_{pump}(\omega') \delta(\omega_0 - \omega') d\omega'. \quad (4)$$

Then we obtain

$$\begin{aligned} E_{sig}(\omega_0 + \Delta) &\propto E_{pump}(\omega_0) \int_{-\infty}^{\infty} E_k(\omega) E_r^*(\omega + \Delta) d\omega \\ &= E_{pump}(\omega_0) \int_{-\infty}^{\infty} |E_k(\omega)| |E_r^*(\omega + \Delta)| e^{i[\Phi_k(\omega) - \Phi_r(\omega + \Delta)]} d\omega. \end{aligned} \quad (5)$$

Therefore, we establish the recognition of matching codes and measuring their period upon the measurement of the codes cross-correlation function in the frequency domain, which is equivalent to the measurement of the spectrum of $E_{sig}(\omega)$. In the case of the finite bandwidth of E_{pump} the measured spectrum of $E_{sig}(\omega)$ represents the cross-correlation function $\xi(k, r, \Delta)$ convoluted with spectral profile of E_{pump} .

Our experimental setup utilizes ultrashort pulses of 65fs (fwhm=15nm) produced by Ti:Sapphire oscillator at 800 nm that were regeneratively amplified at 1KHz rate and splited into three beams. Two beams were passed through the phase-shaping 4f optical set-up incorporated 640-pixel liquid-crystal Spatial Light Modulator which was used to assign different

codes for each beam independently. The corresponding experimental shaping resolution was $\Delta\omega=0.11$ and 0.136 nm/pixel respectively. The third beam was amplitude-shaped using similar 4f shaping set-up to yield narrow [fwhm=0.9nm] spectrum. The resulted three beams were focused at zero delay within the BOXCARS geometrical configuration onto the 1mm-wide piece of fused silica. The resulted spatially isolated signal was collected and its spectrum was measured by CCD camera coupled to the spectrometer with resolution of 0.1nm. It worth noting that alternatively to the presented BOXCARS geometry, polarization gating or self-diffraction geometries can be implemented within the same general formalism.

We have used the quaternary [$p=4$] codes which belong to the nested families $S(0)$ and $S(1)$ and generated using corresponding linear shift registers constructed upon the primitive polynomial. The chosen period of the codes was $L = 2^l - 1=7$, where $l=3$ is the order of the generating polynomial. The size of the family $S(0)$ is $M = L+2=9$ with $|C_{max}|=\sqrt{L+1}+1\simeq 3.8$. The size of the family $S(1)$ is $M = (L+2)(L+1)=64$. Formally, the corresponding value of C_{max} for this case $|C_{max}|=2\sqrt{L+1}+1\simeq 6.66$, however, for the specific case of $l=3$, occurrence of this value is zero and the effective $|C_{max}|=5$.

On Figure 1 the typical spectrum of $E_{sig}(\omega)$ is shown for the cases of $k = r$, and $k \neq r$. The very pronounced peaks observed in the spectrum correspond to the constructive interference between the photoinduced pathways associated with the identical codes, where $k = r$. The peaks are separated by $\Delta_L = n\Delta\omega L$, where n - is the integer parameter. This is in high contrast to the spectrum obtained for the case of the destructive interference among the pathways for the case of different codes, i.e. $k \neq r$. For the peaks exceeding the certain threshold, the distances between the peaks is used for the determination of the code period corresponding to different values of n . The corresponding results for the codes belong to the families $S(0)$ and $S(1)$ are shown on Figure 2 in the form of 2D histogram, where x -axis corresponds to the programmed code period and the y -axis – to the retrieved period. We have successively recognized periods of 98% out of total 432 different periodic codes. As it is seen from Figure 2 the origin of the 2% of the false recognized codes comes from the shortest and longest periods examined. For the shortest period, the factor limiting the recognition power is the actual width of the probe pulse, while its convolution smears the spectral features and broadens the spectrum. On the side of the longest periods, the total spectral width of pulses $E_{k,r}(\omega)$ becomes important. If the pulse bandwidth is not broad

enough, there is not enough constructively interfering pathways provided and the contrast between the cases of $k = r$ and $k \neq r$ is not sufficient for the proper recognition.

The codes with different periods are easily distinguished from the measurement of $E_{sig}(\omega)$ due to the lack of the constructive interference to the amplitude of the emitted signal. For the experimental discrimination between different codes with the same period it is enough to measure the signal at specific frequencies $E_{sig}(\omega_0 + m\Delta_L)$, where $m = 0, 1, \dots$. We present the corresponding results for the code families $S(0)$ and $S(1)$ on the 2D color-map plot of Figure 3 (a) and (b) respectively. Here the color represents the normalized value of $\sum_m E_{sig}(\omega_0 + m\Delta_L)$ for the different pairs of codes k [x -axis] and r [y -axis], so that the auto-correlation cases appear on diagonal. As the signal corresponding to $r = k$ is sufficiently higher than for $r \neq k$, we obtain a very efficient recognition of the 100% of codes belong to $S(0)$ with the signal threshold of 90% [see panel (a)]. For the codes of the $S(1)$ family the value of C_{max} is higher than that of $S(0)$ and, hence, the threshold for the code recognition must be also higher. We obtain 0.6% of experimental false identification using threshold of 95% in this case [see panel (b)] out of the whole set of the cross-correlation measurements. Our experimental results were verified with the numerical evaluation of the spectrum of $E_{sig}(\omega)$ considering experimental parameters as pulse-shaping resolution, bandwidth of the pump pulse, etc. The same fraction of the false identified signals was obtained. We have also performed numerical simulation of the signal considering the pulses with broader bandwidth [fwhm=25nm, pulse duration 45fs], our experimental pulse-shaping resolution, and bandwidth of the pump pulse of fwhm=0.8nm for the $S(1)$ family with $l=4$. Here $L=15$, $M=255$, while $|C_{max}|=9$. For this case we obtain that 100% of codes can be recognized applying the 90% threshold.

In conclusion, we have experimentally demonstrated the all-optical single-shot frequency-domain cross-correlation measurements for the efficient matching and simultaneously measuring the period of low-correlating codes. The presented technique has potential to be implemented in the optical phase-shaped spread-spectrum code division multiple access communication network.

-
- [1] Harte, L., Levine, R., Kikta, R., 3G Wireless Demystified, McGraw-Hill, New York 2002.
 - [2] Pless V. S., Huffman W. C. (Eds.) *Handbook of Coding Theory*. (Elsevier Science B. V.,

Amsterdam, 1998)

- [3] Boztas S., Hammons A. R., & Kumar, P. V. 4-phase sequences with near-optimum correlation properties. *IEEE Trans. Inf. Theory* **38**, 1101 (1992).
- [4] Kumar, P. V., Helleseht T., Calderbank A. R., & Hammons A. R. Large families of quaternary sequences with low correlation. *IEEE Trans. Inf. Theory* **42**, 579 (1996).
- [5] Helleseht T., Kumar P. V. Sequences with low correlation in Pless V. S., Huffman W. C. (Eds.) *Handbook of Coding Theory*. (Elsevier Science B. V., Amsterdam, 1998)
- [6] Prucnal P. R. (Ed.) *Optical Code Division Multiple Access: Fundamentals and Applications* (CRC, Taylor & Francis, Boca Raton, 2006)
- [7] Weiner, A. M., Jiang Z., & Leaird, D. E. Spectrally phase-coded O-CDMA. *J. Opt. Netw.* **6**, 728 (2007) and references therein.
- [8] Weiner, A. M. Femtosecond pulse shaping using spatial light modulators. *Rev. Sci. Inst.* **71**, 1929-1960 (2000).
- [9] Zheng, Z. and Weiner, A. M., Spectral phase correlation of coded femtosecond pulses by second-harmonic generation in thick nonlinear crystals. *Opt. Lett.* **25**, 984 (2000).
- [10] Zheng, Z., Weiner, A. M., Parameswaran, K. R., Chou, M. H., and Fejer, M. M., Low-power spectral phase correlator using periodically poled LiNbO₃ waveguides. *IEEE Photonics Technol. Lett.* **13**, 376 (2001).
- [11] Eckbreth, A. C., BOXCARS: Crossed-beam phase-matched CARS generation in gases. *Appl. Phys. Lett.* **32**, 421 (1978).

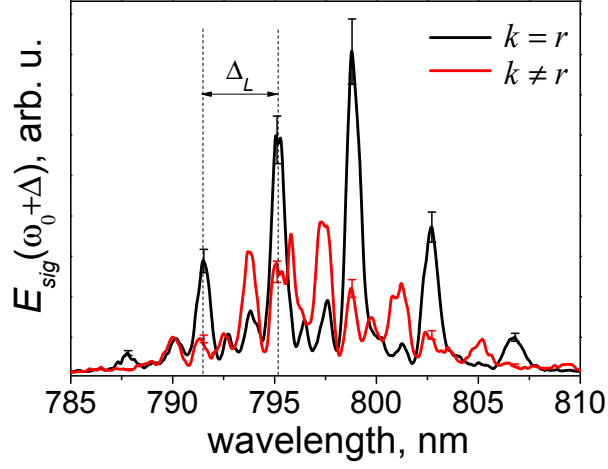


FIG. 1: Typical experimental spectrum of $E_{sig}(\omega)$ for the cases of identical [$k = r$, auto-correlation, black line] and different codes [$k \neq r$, cross-correlation, red line]. The distance between the peaks for the case of $k = r$ corresponds to the period Δ_L .

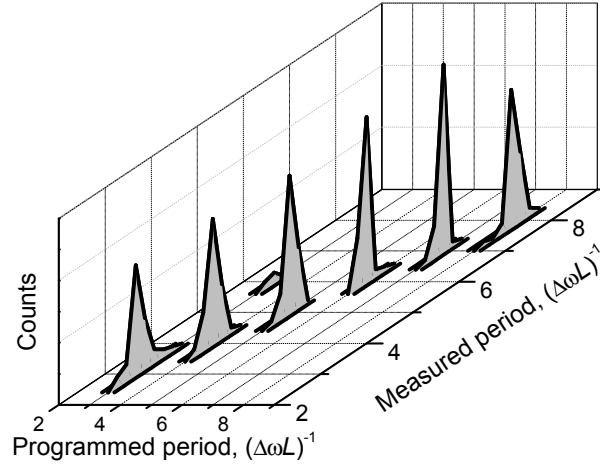


FIG. 2: 2D histogram of measured vs programmed code period Δ_L for 432 different codes belong to family $S(0)$ and $S(1)$. The distribution along the right axis reflects the signal-to-noise experimental ratio, which results in the 98% true matching of the code period.

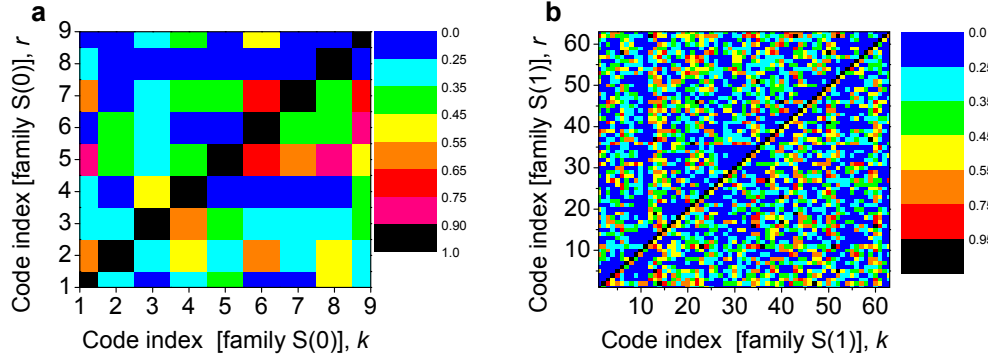


FIG. 3: Color-map plot representing the maximal cross-correlation values $\sum_m E_{sig}(\omega_0 + m\Delta_L)$, $m=0,1,\dots$ for different codes. (a) - results for the family $S(0)$, $l=3$. 100% of the codes was efficiently matched based upon the cross-correlation measurements applying the threshold of 10%. (b) - family $S(1)$, $l=3$. Applying the threshold of 95% we obtain that 0.6% out of whole set of measurements led to the false identification. This result agrees with our numerical evaluation considering the experimental parameters.